First-principles calculations of dynamical screened interactions for the transition metal oxides MO (M=Mn, Fe, Co, Ni)

R. Sakuma and F. Aryasetiawan

Department of Physics, Division Mathematical Physics, Lund University, Sölvegatan 14A 223 62 Lund, Sweden

(Received 14 January 2013; revised manuscript received 13 March 2013; published 11 April 2013)

To facilitate reliable and accurate modeling of the late transition metal oxides from first principles, we present detailed and systematic calculations of the dynamical screened Coulomb interactions (Hubbard U) of MnO, FeO, CoO, and NiO within the constrained random-phase approximation. The matrix elements of the screened interactions are calculated in maximally localized Wannier functions. We consider the screened interactions not only for conventional models that include only the d-like bands but also for models that include both the transition metal d bands and the oxygen p bands. The screened interaction is found to be sensitive to the screening channels subtracted from the polarization function. The frequency dependence of the screened interactions of these oxides is characterized by the two sharp peaks in low-energy region that may be called "subplasmons," which arise from the particle-hole transitions between d and oxygen p states.

DOI: 10.1103/PhysRevB.87.165118 PACS number(s): 71.20.Be, 71.27.+a

I. INTRODUCTION

It is generally agreed that usual band-structure calculations within an effective one-particle approximation such as the local-density approximation (LDA) are insufficient to describe the electronic structure of so-called strongly correlated materials, where very localized states form narrow bands across the Fermi energy. The key parameter characterizing these systems is the so-called Hubbard U, the effective Coulomb interaction acting on these localized states of interest. The approaches taking into account this interaction, such as LDA + U (Ref. 1) and LDA + dynamical mean-field theory (DMFT),[2,3] significantly improve the description of these systems. In early calculations, U was an adjustable parameter and its value was chosen to reproduce experimental spectra. To overcome this drawback, several approaches have been proposed to determine the U parameter from first-principles. One of the earliest is due to Herring[4] who estimated U from atomic data. A similar technique was employed by Cox *et al.*[5] and Herbst *et al.*[6,7] to calculate U for transition metals and rare earths, respectively. Dederichs *et al.*[8] used a constrained LDA (cLDA) method which was later improved by Hybertsen *et al.*[9] by taking into account the change in the kinetic energy of the electrons. A similar approach is due to Cococcioni and de Gironcoli[10] based on linear response theory within the framework of cLDA, which has also been used with success and allows for a self-consistent calculation of U in the LDA + U scheme. A cLDA approach using a supercell calculation,[11–13] where hopping integrals from the orbital with localized electrons is cut off for the central atom in the supercell, has been widely used to calculate U from first principles. In the present work we use the constrained random-phase approximation (RPA),[14] a method which can exclude any screening channels selectively depending on the model considered, and also take into account dynamical or frequency-dependent screening effects,[14] which are found to be important for the renormalization of the quasiparticle bands.[17–19] A precursor to the cRPA method may be found in earlier works.[15,16] The cRPA method has been applied to various systems ranging from graphene[20] to high-temperature Cu-oxide superconductors.[21]

As discussed in previous works,[21–23] the value of the interaction parameters depends on the choice of the "downfolded" model, namely, the orbitals treated in the model as well as the basis functions employed, as the screened interaction is determined by the various screening processes that are not considered in the model. Therefore a careful analysis is needed to make a proper model and choose appropriate parameters. The aim of the present work is to study how the choice of the model affects the value of the static screened interaction as well as its dynamic properties. We study the screened interactions of the late transition metal oxides (TMOs). These materials are prototype of charge-transfer insulators where the correlation effects between the localized states play a key role; due to the hybridization between d and oxygen p states the late TMOs are categorized to charge-transfer insulators[24] rather than Mott-Hubbard insulators, and one cannot neglect the interaction between d-p states. Although modern one-particle approaches, such as the GW approximation, the self-interaction correction, and hybrid functionals, can describe the insulating states of these materials by assuming the antiferromagnetic spin order,[25–29] describing the insulating mechanism in the high-temperature paramagnetic phase requires theories beyond one-particle approximations.

In this work we estimate the screened interaction in the paramagnetic phase of the TMOs in three different models, where a different set of states is excluded from the polarization function. Our emphasis in this work is to analyze the underlying various screening channels that affect static and dynamical properties of the screened interaction. In the present work we do not address the issue of self-consistency, as done in previous works where the constrained RPA is combined with the LDA + U assuming the antiferromagnetic spin order.[30,31] The paramagnetic phase is a natural starting point for model calculations such as the LDA + DMFT where an insulating state is reproduced while maintaining the paramagnetic phase without breaking spin symmetry. We employ the maximally localized Wannier functions[32,33] as basis functions for the localized states due to their flexibility, but another basis can be used, such as the Nth-order muffin-tin-orbital (NMTO) approach.[34] The results are compared with pure transition

metals (TMs), and we estimate the effective interactions between d electrons as well as the effective interatomic interactions between the d electrons of the transition metal and the p electrons of the oxygen, i.e., d-p parameters. The interaction parameters are found to be sensitive to the states excluded in the particle-hole excitations in the polarization function although the d bands are well separated from the rest of the bands. Frequency dependence of the screened Coulomb interactions are also discussed.

II. METHODS

A. Constrained RPA

Since the cRPA method is well described in Refs. 14, 35, and 36, here we only summarize the main points of the approach. The approach starts by dividing the full polarization function P as

$$P = P_{\text{model}} + P_{\text{rest}}, \tag{1}$$

where P_{model} is the polarization involving only the states of interest, such as narrow d bands near the Fermi energy that will be treated in a model Hamiltonian, and P_{rest} contains all other transitions. In previous works,[35,36] P_{model} and P_{rest} are called P_d and P_r, respectively. Within the RPA, P_{model} is calculated as

$$\begin{aligned} &P_{\text{model}}(\mathbf{r},\mathbf{r}';\omega) \\ &= 2\sum_{i\in\text{model}}^{\text{occ.}}\sum_{j\in\text{model}}^{\text{unocc.}} \psi_i^*(\mathbf{r})\psi_j(\mathbf{r})\psi_j^*(\mathbf{r}')\psi_i(\mathbf{r}') \\ &\quad\times\left[\frac{1}{\omega-\epsilon_j+\epsilon_i+i\delta}-\frac{1}{\omega+\epsilon_j-\epsilon_i-i\delta}\right], \end{aligned} \tag{2}$$

where ψ_i and ϵ_i are the eigenfunctions and eigenenergies of a reference one-particle Hamiltonian, which in this work is chosen to be the Kohn-Sham Hamiltonian within the LDA.

The polarization between other electrons as well as between other electrons and the states of interest is calculated as $P_{\text{rest}} = P - P_{\text{model}}$. With this P_{rest}, we can define the "partially" screened Coulomb interaction

$$W_r(\omega) = V + V P_{\text{rest}}(\omega) W_r(\omega) = [1 - V P_{\text{rest}}(\omega)]^{-1} V, \tag{3}$$

where V is the bare Coulomb interaction. The key idea of the cRPA method is that this partially screened interaction W_r may be identified as the Hubbard U or the interaction for the model Hamiltonian:

$$U(\omega) = W_r(\omega), \tag{4}$$

based on the observation that the fully screened interaction W is obtained by screening U with the polarization of the model, P_{model}:

$$\begin{aligned} W(\omega) &= U(\omega) + U(\omega) P_{\text{model}}(\omega) W(\omega) \\ &= [1 - U(\omega) P_{\text{model}}(\omega)]^{-1} U(\omega). \end{aligned} \tag{5}$$

B. Definition of the models

The Hubbard U parameters are determined by specifying the states that will be treated in the model Hamiltonian and the localized basis that describes those states. To illustrate the models considered in this paper, in Fig. 1 we plot the band structure and density of states of TMOs in the paramagnetic phase within the LDA, together with the Wannier-interpolated band structure.[33] The band structure of these systems is characterized by five narrow bands near the Fermi energy, which consist mainly of d orbitals of TMs, and the three broader bands below those d-like bands that consist mainly of oxygen p orbitals. In these systems these d-like and p-like bands are separated from other bands. Since the hybridization of these two orbitals, especially for late TMs, is not negligible, in this work we consider three different models following the notation of Ref. 23:

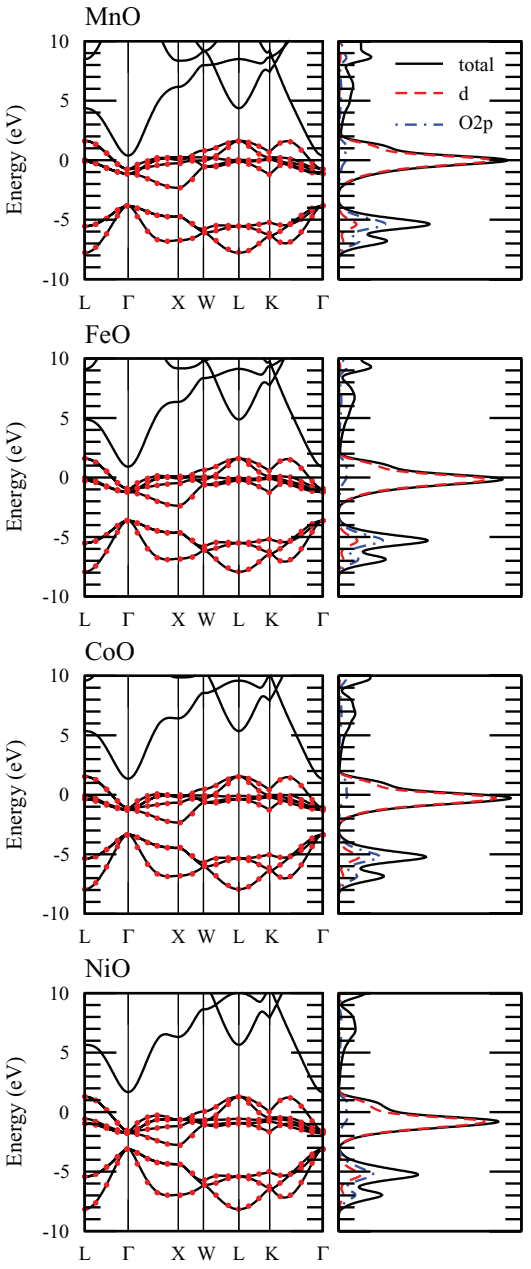

FIG. 1. (Color online) Band structure (left) and density of states (right) of the paramagnetic TMOs calculated with the LDA. In the left panels the Wannier-interpolated band structures[33] are also plotted by circles.

(1) d model: The model consists of five d-like bands near the Fermi energy.

(2) dp model: The model also includes oxygen p bands as well as the five d-like bands.

(3) d-dp model: In this model, the Wannier functions are constructed from d and p bands, but in the cRPA calculations only the polarization between the d bands are subtracted. This corresponds to the case where the one-particle part of the model Hamiltonian consists of d and p states but the Hubbard U is only present in the d bands.

In the d-dp model, due to d-p hybridizations, there is some arbitrariness on how to define the "d contribution," P_{model}, that should be subtracted from the polarization function. In this work we consider the following two approaches:

(1) d-dp model (a) where the five bands near the Fermi energy are regarded as d states and these are subtracted from the polarization.

(2) d-dp model (b) where the d contribution is defined by the projection of each state onto the space spanned by the d-like Wannier functions, as done in Ref. 37. To be specific, for each particle-hole pair $\langle\psi_{\mathbf{k}\mu},\psi_{\mathbf{k}'\nu}\rangle$, where $\psi_{\mathbf{k}\mu}$ is the Kohn-Sham wave function, we calculate the probability in which this pair remain in the d-subspace as

$$p_d(\mathbf{k},\mu;\mathbf{k}',\nu) = \sum_{i\in d}\sum_{j\in d}|S_{\mu i}(\mathbf{k})|^2|S_{\nu j}(\mathbf{k}')|^2, \tag{6}$$

where $S_{\mu i}(\mathbf{k})$ is the Wannier transformation matrix, and we multiply this probability with each particle-hole transition to calculate P_{model}. The Wannier function centered at $\mathbf{R}$ is calculated as

$$w_{n\mathbf{R}} = \frac{1}{N_{\mathbf{k}}}\sum_{\mathbf{k}\mu} e^{-i\mathbf{k}\cdot\mathbf{R}} S_{\mu n}(\mathbf{k})\psi_{\mu\mathbf{k}}(\mathbf{r}). \tag{7}$$

C. Interaction parameters

The matrix elements of the screened Coulomb interaction in the basis of the Wannier functions are expressed as

$$\begin{aligned} &U_{n_1\mathbf{R}_1 n_2\mathbf{R}_2 n_3\mathbf{R}_3 n_4\mathbf{R}_4}(\omega) \\ &= \left\langle w_{n_1\mathbf{R}_1} w_{n_2\mathbf{R}_2}\middle|U(\omega)\middle|w_{n_3\mathbf{R}_3} w_{n_4\mathbf{R}_4}\right\rangle \\ &= \int d^3r d^3r' w^*_{n_1\mathbf{R}_1}(\mathbf{r}) w_{n_2\mathbf{R}_2}(\mathbf{r}) U(\mathbf{r},\mathbf{r}';\omega) \\ &\quad\times w^*_{n_3\mathbf{R}_3}(\mathbf{r}') w_{n_4\mathbf{R}_4}(\mathbf{r}'). \end{aligned} \tag{8}$$

In this work, we discuss the "diagonal" Coulomb parameters for d and p orbitals in the same unit cell, which are defined as

$$U_n(\omega) = \langle w_{n\mathbf{0}} w_{n\mathbf{0}}|U(\omega)|w_{n\mathbf{0}} w_{n\mathbf{0}}\rangle, \tag{9}$$

and "off-diagonal" matrix elements between two different orbitals,

$$U_{nn'}(\omega) = \langle w_{n\mathbf{0}} w_{n\mathbf{0}}|U(\omega)|w_{n'\mathbf{0}} w_{n'\mathbf{0}}\rangle \quad (n\neq n'). \tag{10}$$

Other important matrix elements are the exchange interactions, which are defined as

$$J_{nn'}(\omega) = \langle w_{n\mathbf{0}} w_{n'\mathbf{0}}|U(\omega)|w_{n'\mathbf{0}} w_{n\mathbf{0}}\rangle. \tag{11}$$

The values shown in this paper are the averaged values over five d and three p functions. The full list of these parameters is shown in the Appendix.

D. Computational details

The calculations in this work are based on the full-potential linearized augmented plane-wave (FLAPW) method. We use the DFT code FLEUR (Ref. 38) to calculate the LDA band structures and the GW code SPEX (Ref. 39) to calculate the polarization function and the screened interaction. Inside the FLEUR code, the maximally localized Wannier functions are calculated by using the Wannier90 library.[40,41] All calculations are done without spin polarization, and the lattice parameters taken from Ref. 28 for TMOs and Ref. 42 for TMs except Mn, in which the fcc structure is used.[43] For the LDA exchange-correlation functional, the Perdew-Zunger parametrization[44] is used. For the TMs, we construct the maximally localized Wannier functions using the energy windows presented in Ref. 35. In the constrained RPA calculations, $8\times8\times8$ k points are used in both TMOs and TMs, and around 100 and 50 unoccupied states are included in the polarization function for TMOs and TMs, respectively. To calculate P_{model} for TMs in which the d bands are entangled with other bands, we use two approaches proposed in Refs. 36 and 37.

III. RESULTS AND DISCUSSION

A. Static values

1. Bare Coulomb interaction and spread of the Wannier functions

First we discuss the values of the on-site bare Coulomb interactions, which are solely determined by the localization of the Wannier functions. In Figs. 2(a) and 2(b), we show the diagonal matrix elements of the bare Coulomb interaction

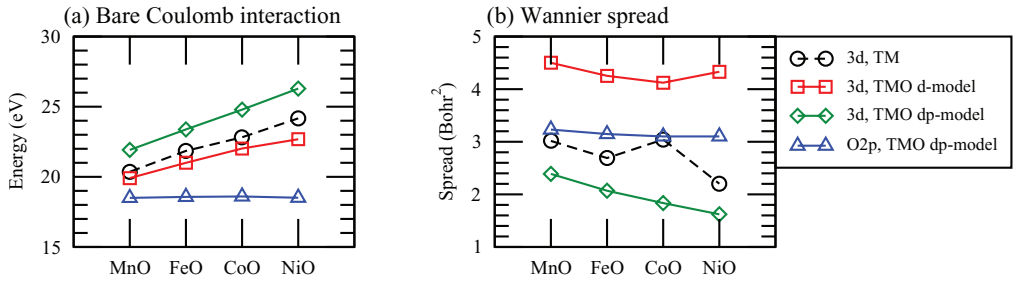

FIG. 2. (Color online) (a) Diagonal part [Eq. (9)] of the bare Coulomb interaction matrix in the Wannier function basis for each model. (b) Spread of the Wannier functions.

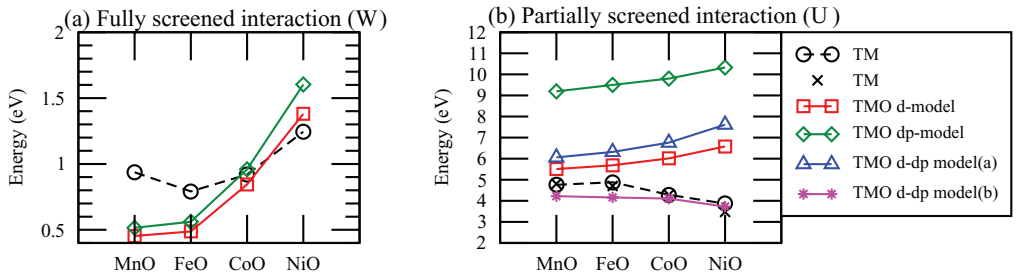

FIG. 3. (Color online) (a) Fully screened Coulomb interaction W of $3d$ Wannier functions. (b) Partially screened Coulomb interaction U of $3d$ Wannier functions. The values for the transition metals (TMs) are calculated with the methods in Refs. 36 and 37 for open circles and crosses, respectively.

averaged over five and three Wannier functions of, respectively, d and p orbitals in TMOs, and the spread of the Wannier functions.[32] The results for the pure TMs are also shown for comparison. The overall trend of these quantities is as expected: the d-like Wannier functions in the dp model, which are constructed with larger energy windows and hence more localized, yield the largest bare Coulomb interaction. The values of the Coulomb interaction in the d model are smaller than the corresponding values for the pure TMs, since the five d-like Wannier functions in the d model contain some oxygen $2p$ states and are less localized. As the atomic number of the transition metal of the TMOs increases, the attractive Coulomb interaction between nuclei and electrons gets stronger and electrons become more localized to the atoms. This leads to the increase of the Coulomb interaction and localization of the Wannier functions, as seen in Fig. 2(b), although it should be noted that the spread of the Wannier functions is mainly determined by the tails of the functions and is sensitive to the choice of the energy windows and the number of k points used. On the other hand, the bare Coulomb interactions and the spread for oxygen $2p$ Wannier functions do not depend very much on the systems considered, indicating that the oxygen bands are essentially the same in different TMOs.

2. *d-d interaction*

In Fig. 3(a) we plot the diagonal matrix elements of the fully screened interaction $W(\omega = 0)$ for the d-like Wannier functions of TMOs in the d model and the dp model, together with the results of pure TMs. As can be seen, as one goes from MnO to NiO, the fully screened interaction W monotonically increases by $\approx$1 eV, while TMs show a smaller change. The difference between the results in the d and dp models is around 0.2 eV, which is much smaller than the difference in the bare Coulomb interaction. The difference in the degree of localization of the Wannier functions has a much smaller absolute effect in W than in the bare Coulomb interaction. This is understandable because the screened interaction W decays faster with distance compared to the bare interaction due to the screening. However, the percentage difference between the screened interactions W of the two models is almost the same as the one for the bare interactions.

In Fig. 3(b) the results of the partially screened interaction $U(\omega = 0)$ are plotted for various models. In the case of pure TMs, the two approaches proposed in Refs. 36 and 37 are used, and these two approaches are found to yield similar results for the late TMs. In contrast to W, the values of U are quite sensitive to the choice of the models. There are two possible factors that determine the value of U: one is the localization of the d Wannier functions that give large contributions to the values of the bare interactions as seen in Fig. 2(a), and the other is the polarization $P_{\rm rest}$. As expected, the dp model yields the largest U as this model takes out a large part of the particle-hole excitations involving the d and p states from the polarization function. The d model and d-dp model (a) take out the same d-like contributions from the polarization function, so the difference between the results in these two models can be traced to the localization of the Wannier functions. Indeed, since the Wannier functions of the d-dp model are more localized than those of the d model, the U values of the former are larger than the latter. In the d, dp, and d-dp (a) models, the values of U increase monotonically from MnO to NiO and this tendency could be explained by the increase localization of the d Wannier functions.

The d-dp model (b), however, exhibits a somewhat different tendency compared to other models. This model yields the smallest U ($\approx$4 eV), and as the atomic number of the TMs increases the value of U slightly decreases, while in other three models the value of U increases. This tendency is closer to the results of the pure TMs which may be explained by considering the remaining polarization, $P_{\rm rest}$. In the other three models, the polarization involving the d-like bands that cross the Fermi level is completely removed from $P_{\rm rest}$ so that $P_{\rm rest}$ is "insulatorlike,"while in the d-dp model (b), due to the d-p hybridization some metallic screening remains in $P_{\rm rest}$ after the d contribution is subtracted. For this reason, U in the d-dp model (b) is smaller than in the d-dp model (a) because, due to some remaining metallic screening, the Coulomb interaction is more efficiently screened in the former model than in the latter. In this respect, the d-dp model (b) is similar to the case of the pure TMs and the results are therefore closer to the case of the TMs.

3. *p-p interaction and d-p interaction*

In Fig. 4, we show the values of the diagonal screened interaction parameters in the basis of oxygen $2p$-like Wannier functions. Interestingly, the matrix elements of W for the oxygen $2p$ states, which are $\approx$3 eV for all TMOs, are found to be larger than those of $3d$ orbitals [Fig. 3(a)]. This somewhat

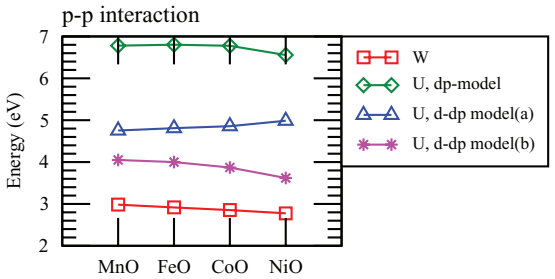

FIG. 4. (Color online) Fully screened interaction (W) and partially screened interaction U of oxygen $2p$-like Wannier functions.

counterintuitive result can be explained by considering the physical significance of $W(\mathbf{r},\mathbf{r}';\omega)$, which is the screened interaction at $\mathbf{r}'$ arising from a point charge located at $\mathbf{r}$. If a hole is created on the oxygen site, this hole is not as effectively screened as a hole created on the transition metal site because electrons occupying the oxygen $2p$ bands need a lot more energy to be polarized than electrons occupying the transition metal d bands. The oxygen $2p$ bands are located deeper in energy than the transition metal d bands so that more energy is needed to excite electrons occupying the p bands than the d bands. The variation of p-p interaction over materials is smaller than the case in the d-d interaction. In the dp model, in which the p orbitals are treated on equal footing to d states, the interaction between p states, U_{pp}, is around 7 eV, which is comparable to U_{dd} ($\sim$10 eV). In Fig. 4 we also show p-p interactions in d-dp models (a) and (b), although in these models the interactions between the p states are not to be included. In these cases the difference between U_{pp} and U_{dd} is even smaller; this is another indication of the importance of choosing proper models and excluding proper screen channels.

In Fig. 5 we plot the interatomic interactions between d and p states. In the case of the fully screened interaction W and in the d-dp model (b), the interaction between d and p states is negligible, while the partially screened interactions U is around 1 eV in other models. This qualitative difference is again due to the nature of the remaining polarization function P_{rest}; in the d-dp model (b), the polarization is metalliclike and the interaction rapidly decays with distance, while in other models the polarization is insulatorlike and the interaction is more long ranged.

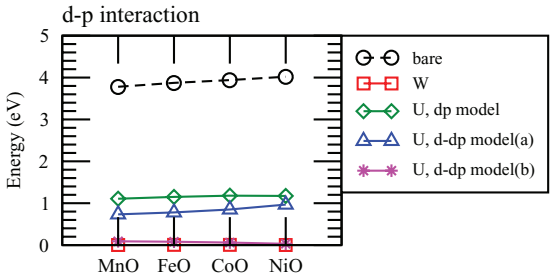

FIG. 5. (Color online) Fully screened interaction (W) and partially screened interaction U between d and $2p$ Wannier functions.

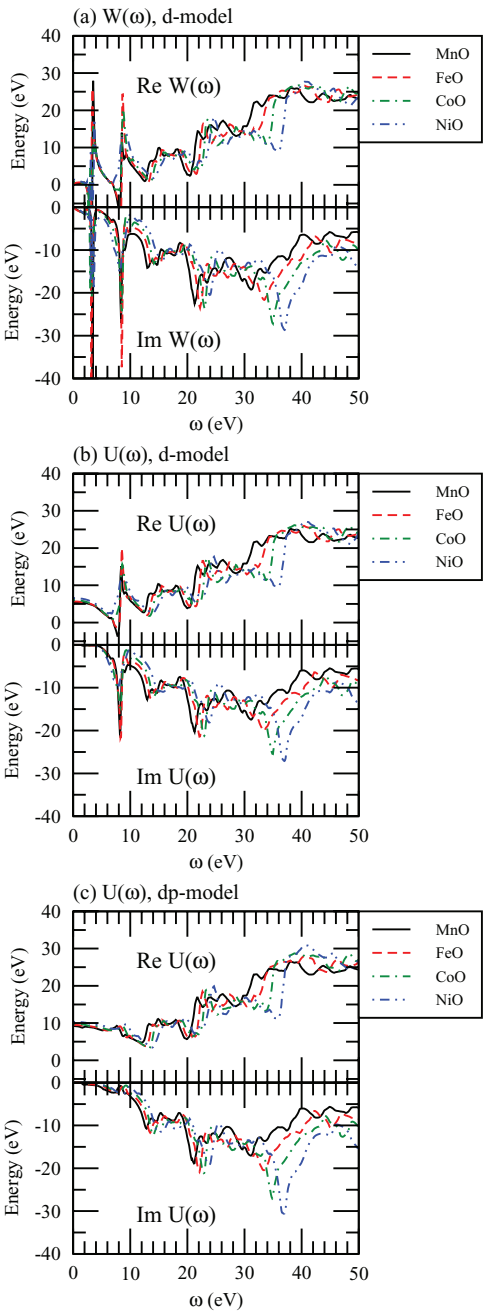

FIG. 6. (Color online) (a) Fully screened interaction [$W(\omega)$] in the d model. (b) Partially screened interaction [$U(\omega)$] in the d model. (c) Partially screened interaction [$U(\omega)$] in the dp model.

4. Comparison with other works

Among the late TMOs, the value of the Hubbard U parameter for NiO is intensively investigated. The value of 5–8 eV is deduced from the constrained LDA[13,45–47] and a supercell calculation,[48] and $U = 8$ eV is used in LDA + DMFT calculations.[49–53] These values are similar to our results in the d model and the d-dp model (a), in which the five d-like bands near the Fermi energy (Fig. 1) are subtracted from the polarization. As we discussed above, due to the metallic contribution of the polarization P_{rest}, the value evaluated in the d-dp model (b), in which the d contribution of the polarization

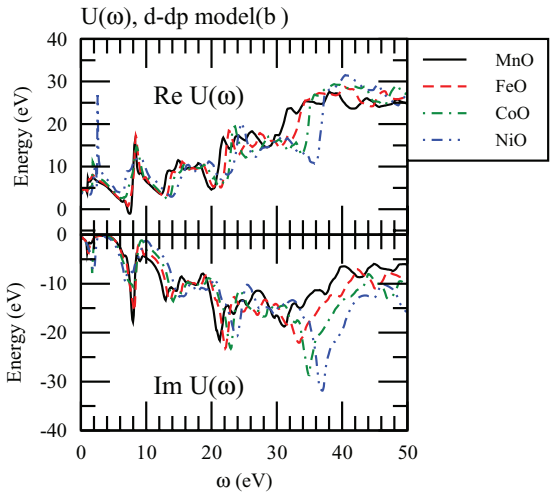

FIG. 7. (Color online) Partially screened interaction $[U(\omega)]$ in the d-dp model (b).

is calculated from the projection, is considerably smaller than the value obtained in either the d model or the d-dp model.

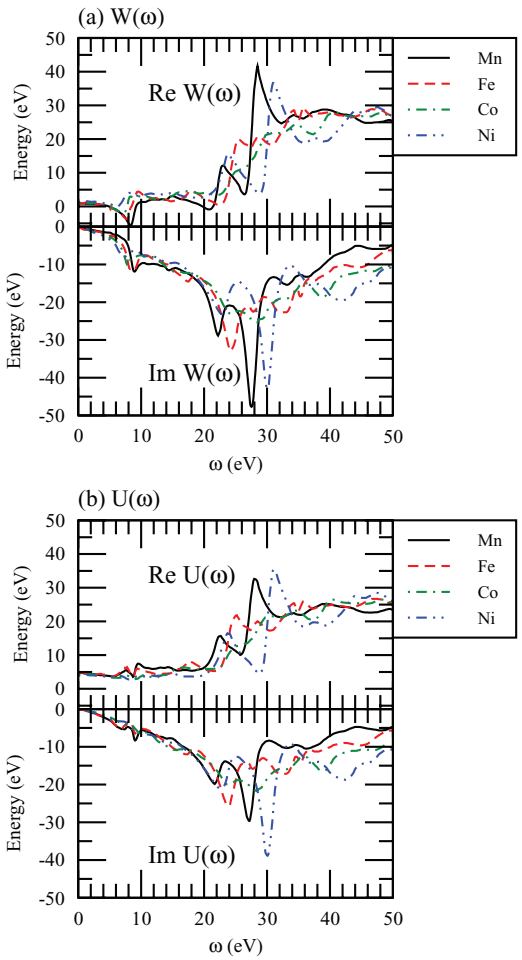

FIG. 8. (Color online) (a) Fully screened interaction $[W(\omega)]$ of the transition metals. (b) Partially screened interaction $[U(\omega)]$ of the transition metals.

Recently Karlsson *et al*. and Shih *et al*. calculated the value of U of antiferromagnetic NiO self-consistently by combining the constrained RPA with LDA + U,[30,31] and both obtained a similar result of 6.6 eV. The work of Shih *et al*. is based on the projection approach, similar to our d-dp model (b), but nevertheless their calculated value of U is large. Their large value can be explained by a large gap (∼3 eV) in the initial self-consistent one-particle states used in the constrained RPA calculation, giving an insulatorlike $P_{\rm rest}$. In the paramagnetic phase, however, the insulating state cannot be obtained within a one-particle approximation and one inevitably has to perform calculations in the metallic state. In this sense, the other two models, the d-model and d-dp model (a), yield more sensible results, since in these models all the low-energy excitations are removed so that the polarization $P_{\rm rest}$ is insulatorlike, similar to the works of Karlsson *et al*. and Shih *et al*.

B. Frequency dependence

Next we discuss the frequency dependence of the screened interaction, which reflects the band structure of the systems through the polarization function. In Figs. 6(a)–6(c), we plot the frequency dependence of the fully screened interaction $W(\omega)$ in the d model and the partially screened interaction $U(\omega)$ in the d and dp models. For comparison, $W(\omega)$ and $U(\omega)$ in the d-dp model (b) and for the transition metals are also shown in Figs. 7(a) and 7(b) and 8(a) and 8(b).

A striking feature of $W(\omega)$ in TMOs is two sharp peak structures at around 3 and 8 eV. By comparing $W(\omega)$ in Fig. 6(a) and partially screened interactions $U(\omega)$ in the d and dp models in Figs. 6(b) and 6(c), one can see that the first peak at around 3 eV originates from the polarization among the d states, while the second peak at around 8 eV comes from the polarization involving the d-p transition. Similar sharp peaks in the low-energy region are also seen in VO_2,[54] as well as $4f$ materials,[55,56] and this seems to be characteristic of the correlated materials. These peaks originate from the particle-hole excitations between the localized states and may be qualitatively understood by considering a simple two-level model;[57] in this model, the peak position of Im$W(\omega)$ is given by

$$\Omega_{nn'} = \sqrt{\Delta_{nn'}^2 + 2J_{nn'}\Delta_{nn'}}, \tag{12}$$

where $\Delta_{nn'}$ is the energy difference between two states n and n', and $J_{nn'}$ is the static value of the screened exchange interaction [Eq. (11)] between them. In the TMOs considered in this work, $\Delta_{dd} \approx 3, \Delta_{dp} \approx 7$, $J_{dd} \approx 0.7$, and $J_{dp} \approx 0$. Equation (12) shows that the two peaks are essentially the

TABLE I. The interaction parameters in the d model.

	MnO	FeO	CoO	NiO
U	5.5	5.7	6.0	6.6
$U_{t_{2g}}$	5.7	5.9	6.3	7.0
U_{e_g}	5.3	5.4	5.6	6.0
U'	4.2	4.3	4.6	5.1
J	0.6	0.7	0.7	0.7

TABLE II. The interaction parameters in the dp model.

	MnO	FeO	CoO	NiO
U	9.2	9.5	9.8	10.3
$U_{t_{2g}}$	8.9	9.2	9.5	10.0
U_{e_g}	9.7	10.0	10.3	10.8
U'	7.7	7.9	8.1	8.6
J	0.7	0.8	0.8	0.9
U_p	6.8	6.8	6.8	6.6
U'_p	5.4	5.5	5.4	5.2
J_p	0.7	0.7	0.6	0.6
U_{dp}	1.1	1.2	1.2	1.2

TABLE IV. The interaction parameters in the d-dp model (b).

	MnO	FeO	CoO	NiO
U	4.2	4.2	4.1	3.7
$U_{t_{2g}}$	4.1	4.1	4.2	4.0
U_{e_g}	4.4	4.3	4.0	3.4
U'	2.8	2.7	2.6	2.2
J	0.7	0.7	0.8	0.8
U_p	4.1	4.0	3.9	3.6
U'_p	2.8	2.7	2.6	2.4
J_p	0.6	0.6	0.6	0.6
U_{dp}	0.1	0.1	<0.1	<0.1

particle-hole excitation between two localized states modified by the interaction term. These peaks are given by the poles of the inverse dielectric function, and hence these are collective excitations that may be called "subplasmons." In the TMOs considered here the position of these two sharp peaks is rather material independent, as the band structure of them is similar, while the position of the plasmon peaks seen in $\mathrm{Im}W(\omega)$ and $\mathrm{Im}U(\omega)$ in Figs. 6–8 depends on materials.

By comparing Figs. 6(b) and 7 it becomes clear that in the d-dp model (b) there is significant remaining contribution to the P_{model} from the excitations between the d-like bands near the Fermi energy, especially for NiO, in which the d-p hybridization is strong. This structure in $\mathrm{Im}U(\omega)$ affects the static value of the screened interaction through the Kramers-Kronig relation and yields smaller U, as discussed above. We note again that as in reality the TMOs have large gaps due to many-body effects, which shift these d-d peaks towards higher energy and therefore modify the static and dynamical properties of U, a proper treatment would require including the vertex correction to the RPA.[58,59] This point will be investigated in future work.

IV. SUMMARY

In this paper we have performed a detailed investigation on the dynamical screened Coulomb interaction for the paramagnetic phase of the late transition metal oxides within the constrained RPA. The screened interaction acting on the d states shows a different trend depending on which screening channels are subtracted from the polarization function, reflecting the properties of the remaining polarization function P_{rest}. The interaction parameters between the oxygen p states as well as d-p interactions are also calculated. We have also calculated the frequency-dependent screened interactions and found two distinct peaks in the low-energy region, which are due to transitions involving d and p states. It would be interesting to investigate how this low-energy structure of $U(\omega)$ will affect the renormalization of the d states compared to usual LDA + DMFT calculations with static U.

TABLE III. The interaction parameters in the d-dp model (a).

	MnO	FeO	CoO	NiO
U	6.1	6.3	6.8	7.6
$U_{t_{2g}}$	6.0	6.2	6.7	7.5
U_{e_g}	6.2	6.5	6.9	7.7
U'	4.6	4.8	5.2	5.9
J	0.7	0.8	0.8	0.9
U_p	4.8	4.8	4.9	5.0
U'_p	3.5	3.5	3.6	3.7
J_p	0.6	0.6	0.6	0.6
U_{dp}	0.7	0.8	0.9	1.0

ACKNOWLEDGMENTS

We would like to thank C. Friedrich and S. Blügel for providing us with their FLAPW code. This work was supported by Swedish Research Council.

APPENDIX: INTERACTION PARAMETERS

Here we list the screened interaction parameters of the transition metal oxides and also for the transition metals. In Tables I–V, U, U', and J are the average values of diagonal [Eq. (9)], off-diagonal [Eq. (10)], and exchange [Eq. (11)] interactions between d Wannier functions, and U_p, U'_p, and J_p are the corresponding values for oxygen p functions. For the transition metal oxides we also show the diagonal interaction of t_{2g} and e_g states ($U_{t_{2g}}$ and U_{e_g}). The interaction between d and p states is denoted by U_{dp}.

TABLE V. The interaction parameters in the transition metals.

		Mn	Fe	Co	Ni
Method of Ref. 36	U	4.8	4.9	4.3	3.9
	U'	3.5	3.5	2.9	2.5
	J	0.6	0.7	0.7	0.7
Method of Ref. 37	U	4.8	4.7	4.3	3.5
	U'	3.6	3.4	2.9	2.1
	J	0.6	0.7	0.7	0.7

[1] V. I. Anisimov, J. Zaanen, and O. K. Andersen, Phys. Rev. B **44**, 943 (1991).
[2] A. Georges, G. Kotliar, W. Krauth, and M. J. Rozenberg, Rev. Mod. Phys. **68**, 13 (1996).
[3] G. Kotliar, S. Y. Savrasov, K. Haule, V. S. Oudovenko, O. Parcollet, and C. A. Marianetti, Rev. Mod. Phys. **78**, 865 (2006).
[4] C. Herring, in *Magnetism*, edited by G. T. Rado and H. Suhl, Vol. 4 (Academic, New York, 1966).
[5] B. N. Cox, M. A. Coultard, and P. Loyd, J. Phys. F **4**, 807 (1974).
[6] J. F. Herbst, R. E. Watson, and J. W. Wilkins, Phys. Rev. B **13**, 1439 (1976).
[7] J. F. Herbst, R. E. Watson, and J. W. Wilkins, Phys. Rev. B **17**, 3089 (1978).
[8] P. H. Dederichs, S. Blügel, R. Zeller, and H. Akai, Phys. Rev. Lett. **53**, 2512 (1984).
[9] M. S. Hybertsen, M. Schlüter, and N. E. Christensen, Phys. Rev. B **39**, 9028 (1989).
[10] M. Cococcioni and S. de Gironcoli, Phys. Rev. B **71**, 035105 (2005).
[11] A. K. McMahan, R. M. Martin, and S. Satpathy, Phys. Rev. B **38**, 6650 (1988).
[12] O. Gunnarsson, O. K. Andersen, O. Jepsen, and J. Zaanen, Phys. Rev. B **39**, 1708 (1989).
[13] V. I. Anisimov and O. Gunnarsson, Phys. Rev. B **43**, 7570 (1991).
[14] F. Aryasetiawan, M. Imada, A. Georges, G. Kotliar, S. Biermann, and A. I. Lichtenstein, Phys. Rev. B **70**, 195104 (2004).
[15] M. Springer and F. Aryasetiawan, Phys. Rev. B **57**, 4364 (1998).
[16] T. Kotani, J. Phys.: Condens. Matter **12**, 2413 (2000).
[17] P. Werner and A. J. Millis, Phys. Rev. Lett. **104**, 146401 (2010).
[18] M. Casula, A. Rubtsov, and S. Biermann, Phys. Rev. B **85**, 035115 (2012).
[19] M. Casula, P. Werner, L. Vaugier, F. Aryasetiawan, T. Miyake, A. J. Millis, and S. Biermann, Phys. Rev. Lett. **109**, 126408 (2012).
[20] T. O. Wehling, E. Şaşıoğlu, C. Friedrich, A. I. Lichtenstein, M. I. Katsnelson, and S. Blügel, Phys. Rev. Lett. **106**, 236805 (2011).
[21] A. Kozhevnikov, A. G. Eguiluz, and T. C. Schulthess, in *SC'10 Proceedings of the 2010 ACM/IEEE International Conference for High Performance Computing, Networking, Storage, and Analysis* (IEEE Computer Society, Washington, DC, 2010), pp. 1–10.
[22] J. M. Tomczak, T. Miyake, and F. Aryasetiawan, Phys. Rev. B **81**, 115116 (2010).
[23] L. Vaugier, H. Jiang, and S. Biermann, Phys. Rev. B **86**, 165105 (2012).
[24] J. Zaanen, G. A. Sawatzky, and J. W. Allen, Phys. Rev. Lett. **55**, 418 (1985).
[25] S. V. Faleev, M. van Schilfgaarde, and T. Kotani, Phys. Rev. Lett. **93**, 126406 (2004).
[26] A. Svane and O. Gunnarsson, Phys. Rev. Lett. **65**, 1148 (1990).
[27] Z. Szotek, W. M. Temmerman, and H. Winter, Phys. Rev. B **47**, 4029 (1993).
[28] F. Tran, P. Blaha, K. Schwarz, and P. Novák, Phys. Rev. B **74**, 155108 (2006).
[29] C. Rödl, F. Fuchs, J. Furthmüller, and F. Bechstedt, Phys. Rev. B **79**, 235114 (2009).
[30] K. Karlsson, F. Aryasetiawan, and O. Jepsen, Phys. Rev. B **81**, 245113 (2010).
[31] B.-C. Shih, T. A. Abtew, X. Yuan, W. Zhang, and P. Zhang, Phys. Rev. B **86**, 165124 (2012).
[32] N. Marzari and D. Vanderbilt, Phys. Rev. B **56**, 12847 (1997).
[33] I. Souza, N. Marzari, and D. Vanderbilt, Phys. Rev. B **65**, 035109 (2001).
[34] O. K. Andersen and T. Saha-Dasgupta, Phys. Rev. B **62**, R16219 (2000).
[35] T. Miyake and F. Aryasetiawan, Phys. Rev. B **77**, 085122 (2008).
[36] T. Miyake, F. Aryasetiawan, and M. Imada, Phys. Rev. B **80**, 155134 (2009).
[37] E. Şaşıoğlu, C. Friedrich, and S. Blügel, Phys. Rev. B **83**, 121101 (2011).
[38] http://www.flapw.de/
[39] C. Friedrich, S. Blügel, and A. Schindlmayr, Phys. Rev. B **81**, 125102 (2010).
[40] A. A. Mostofi, J. R. Yates, Y.-S. Lee, I. Souza, D. Vanderbilt, and N. Marzari, Comput. Phys. Commun. **178**, 685 (2008).
[41] F. Freimuth, Y. Mokrousov, D. Wortmann, S. Heinze, and S. Blügel, Phys. Rev. B **78**, 035120 (2008).
[42] C. Kittel, *Introduction to Solid State Physics*, 8th ed. (Wiley, New York, 2005).
[43] C. Jing, S. X. Cao, and J. C. Zhang, Phys. Rev. B **68**, 224407 (2003).
[44] J. P. Perdew and A. Zunger, Phys. Rev. B **23**, 5048 (1981).
[45] S. L. Dudarev, A. I. Liechtenstein, M. R. Castell, G. A. D. Briggs, and A. P. Sutton, Phys. Rev. B **56**, 4900 (1997).
[46] T. Cai, H. Han, Y. Yu, T. Gao, J. Du, and L. Hao, Physica B **404**, 89 (2009).
[47] H. Jiang, R. I. Gomez-Abal, P. Rinke, and M. Scheffler, Phys. Rev. B **82**, 045108 (2010).
[48] M. R. Norman and A. J. Freeman, Phys. Rev. B **33**, 8896 (1986).
[49] X. Ren, I. Leonov, G. Keller, M. Kollar, I. Nekrasov, and D. Vollhardt, Phys. Rev. B **74**, 195114 (2006).
[50] J. Kuneš, V. I. Anisimov, S. L. Skornyakov, A. V. Lukoyanov, and D. Vollhardt, Phys. Rev. Lett. **99**, 156404 (2007).
[51] J. Kuneš, V. I. Anisimov, A. V. Lukoyanov, and D. Vollhardt, Phys. Rev. B **75**, 165115 (2007).
[52] M. Karolak, G. Ulm, T. Wehling, V. Mazurenko, A. Poteryaev, and A. Lichtenstein, J. Electron Spectrosc. Relat. Phenom. **181**, 11 (2010).
[53] I. A. Nekrasov, V. S. Pavlov, and M. V. Sadovskii, JETP Lett. **95**, 581 (2012).
[54] M. Gatti, F. Bruneval, V. Olevano, and L. Reining, Phys. Rev. Lett. **99**, 266402 (2007).
[55] R. Sakuma, T. Miyake, and F. Aryasetiawan, Phys. Rev. B **86**, 245126 (2012).
[56] F. Nilsson, R. Sakuma, and F. Aryasetiawan (unpublished).
[57] F. Aryasetiawan, R. Sakuma, and K. Karlsson, Phys. Rev. B **85**, 035106 (2012).
[58] S. Biermann, F. Aryasetiawan, and A. Georges, Phys. Rev. Lett. **90**, 086402 (2003).
[59] T. Ayral, P. Werner, and S. Biermann, Phys. Rev. Lett. **109**, 226401 (2012).